Bohr Effects of the Partially-Ligated (CN-met) Intermediates of Hemoglobin as Probed by Quaternary Assembly†

Margaret A. Daugherty,‡ Madeline A. Shea,§ and Gary K. Ackers*,‡

Department of Biochemistry and Molecular Biophysics, Washington University School of Medicine, St. Louis, Missouri 63110, and Department of Biochemistry, University of Iowa College of Medicine, Iowa City, Iowa 52242

Received February 18, 1994; Revised Manuscript Received May 31, 1994®

ABSTRACT: Free energies of quaternary assembly (dimers to tetramers) were determined for the 10 ligation species of CN-methemoglobin in the region of the alkaline Bohr effect (pH 7.0–9.5). Analysis of this database yielded the following principal findings: (1) At each pH, the nine CN-met species exhibit two distinct values of Bohr proton release and Bohr free energy. The two Bohr effects are found to distribute in a fashion that coincides with predictions of a symmetry rule (Ackers et al., 1992), i.e., the first value reflects a "tertiary Bohr effect" arising from ligation within the quaternary T tetramer and a second Bohr effect arises from the quaternary transition (T → R) which occurs when both dimeric half-molecules acquire at least one ligated subunit. (2) The Bohr effects for CN-met ligation are in good agreement with previously-established Bohr effects for stepwise O_2 binding under identical conditions (Chu et al., 1984). (3) In combination with recent studies which show that CN-met species [21] has a quaternary T structure (Daugherty et al., 1991; Doyle & Ackers, 1992; LiCata et al., 1993), the present results show that the "tertiary Bohr effect" within quaternary T exceeds the Bohr effect of dissociated dimers, as suggested by Lee and Karplus (1983). (4) The tertiary Bohr effect is found to account for the pH dependence of tertiary constraint energy, ΔG_{tc}, which "pays" for ligand-binding cooperativity prior to the quaternary (T → R) switchover. Possible origins of the tertiary Bohr effect and its relationship to the quaternary Bohr effect are considered.

The allosteric regulation of human hemoglobin derives from the mutually-linked interactions with five small molecules: oxygen, protons, chloride, 2,3-diphosphoglycerate, and carbon dioxide. Interdependencies of the hemoglobin molecule's reactions with these regulatory species must be understood for each of the 10 structurally-unique combinations of ligated and unligated heme sites (Figure 1). This goal has yet to be attained, even though much is known regarding properties of the end-state species [01] and [41] (e.g., from crystallographic structures) and also regarding the average behavior at each stage of oxygenation (e.g., from oxygen-binding isotherms). During the last several years, the differing functional properties of configurational isomers within each degree of ligation (e.g., species [11] vs [12] or [21] vs [22]) have become amenable to systematic study (Smith & Ackers, 1985; Perrella et al., 1990a; Ackers et al., 1992). Our work on this problem is an outgrowth of the realization obtained from analyses of hemoglobin models that experimental information on the intermediate ligation states is critically required for adequately deciphering the hemoglobin allosteric mechanism (Ackers & Johnson, 1981; Johnson & Ackers, 1982; Johnson et al., 1984).

Investigation of the eight intermediate species with oxygenated sites has been precluded due to the extreme lability of the bound oxygen and also the dissociation of tetrameric hemoglobin into dimers. To circumvent these problems, strategies have been developed in which ligands and ligand analogs other than oxygen are used. These approaches take advantage of ligands which bind tightly to the heme, such as CO and NO (Perrella & Rossi-Bernardi, 1981; Perrella et al., 1990a) and CN-met (Smith & Ackers, 1985; Perrella et al., 1990b) or of metal-substituted hemes which mimic normal deoxy Fe(II) heme (e.g., Co(II); Yonetani et al., 1974; Speros et al., 1991) or the normal Fe(II)O_2 heme (e.g., Mn(III); Smith et al., 1987). Cooperativity of heme site ligation is investigated by measuring the thermodynamic linkage to quaternary assembly of the (noncooperative) dimers into tetramers. These measurements yield values for the cooperative free energies, ${}^{ij}\Delta G_c$ (Figure 2).

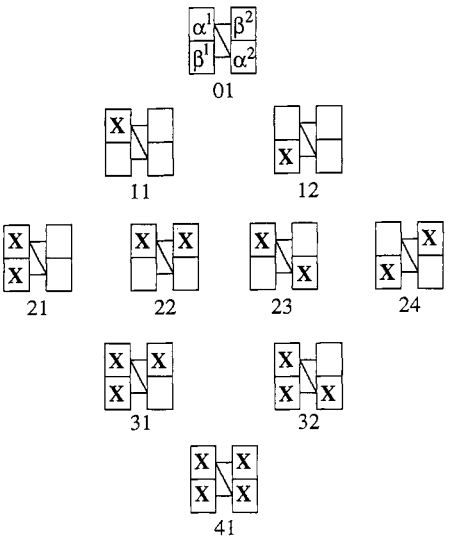

FIGURE 1: Topographic representation of the 10 ligation states of tetrameric hemoglobin. The index *ij* represents each particular species with *i* ligands bound. Subunit positions are shown in species [01]. The solid lines denote intersubunit contacts.

$$ {}^{ij}\Delta G_c = {}^{ij}\Delta G_2 - {}^{01}\Delta G_2 \quad (1)$$

Terms on the right-hand side are free energies of dimer to

† This work was supported by NSF Grant DMB9107244 and NIH Grants R37-GM24486 and HL51084.

* To whom correspondence should be addressed.
‡ Washington University School of Medicine.
§ University of Iowa College of Medicine.

® Abstract published in *Advance ACS Abstracts,* July 15, 1994.

0006-2960/94/0433-10345$04.50/0 © 1994 American Chemical Society

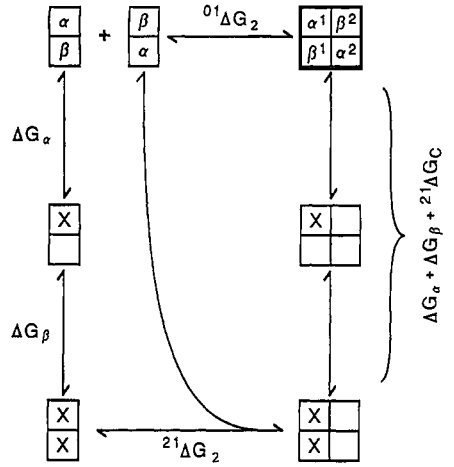

FIGURE 2: Thermodynamic linkage between subunit assembly (horizontal axis) and ligation (vertical axis). ΔG_α and ΔG_β are intrinsic binding energies per site. The expression $(\Delta G_\alpha + \Delta G_\beta + {}^{21}\Delta G_c)$ is the free energy difference between a mole of doubly-ligated tetramers (species [21]) and a mole of unligated tetramers (species [01]). $^{01}\Delta G_2$ is the free energy of forming the unligated tetramer from two unligated dimers. $^{21}\Delta G_2$ is the free energy of forming species [21] by combination of a doubly-ligated dimer and an unligated dimer. By summing the free energies around the thermodynamic cycle, we can write an equation for cooperative free energy in terms of subunit assembly free energies: $^{21}\Delta G_c = {}^{21}\Delta G_2 - {}^{01}\Delta G_2$. Similar relations hold for all nine ligation species.

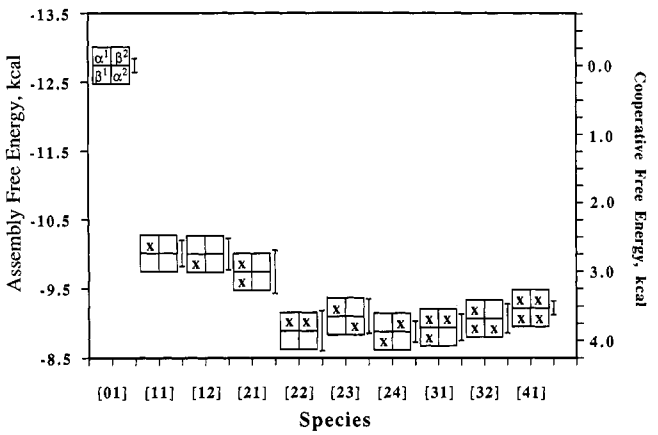

FIGURE 3: Distribution of cooperative free energies for the 10 microstates of cyanomethemoglobin. Conditions are 0.1 M Tris-HCl, 0.1 M NaCl, and 1 mM Na_2EDTA at pH 8.8, 21.5 °C.

tetramer assembly for species [01] and [*ij*]. By thermodynamic linkage, $^{ij}\Delta G_c$ also represents the free energy difference between ligating the tetramer to form species [*ij*] and that of ligating the same sites on dissociated dimers. Figure 2 illustrates the fundamental point that energy-generating structure changes at any location within the tetrameric molecule may contribute to $^{ij}\Delta G_c$, regardless of whether the experimental method used in its determination measures assembly or ligation. The combined usage of both assembly and ligation with structure-specific modification has proved especially powerful in delineating how the cooperativity of heme site ligation is mediated by the dimer–dimer interactions (LiCata et al., 1993).

Initial work at pH 7.4 on the CN-met system (Smith & Ackers, 1983, 1985) revealed that the 10 microstates distribute with three cooperative free energies and that the doubly-ligated species segregate in a combinatorial fashion into two distinct levels (see Figure 3). Subsequent work (Perrella et al., 1990) verified the combinatorial nature of this distribution while showing that species [22] distributes with species [23] and [24] rather than with species [21] where it was initially assigned. The same tripartite distribution was also determined for the Fe(II)/Mn(III) system (Smith et al., 1987; Ackers, 1990) with species [21] at the level of the singly-ligated molecules while species [22], [23], and [24] occupied a separate level with species [31], [32], and [41]. Both of these systems appeared to represent simplified cases of a more complex five-level energetic distribution found with the Co(II)/Fe(II)CO system (Speros et al., 1991). A surprising common feature of these ligation systems was that the doubly-ligated tetramers always distribute into two different cooperative free energies. This precludes even a most general form of the classical two-state MWC model (Monod et al., 1965) and requires a minimum of three "allosteric states" (Ackers, 1990). The "third allosteric state" was not postulated as necessarily different in quaternary structure from either of the well-known T and R forms defined crystallographically (Perutz, 1970; Baldwin & Chothia, 1979). It was proposed alternatively to reflect tertiary conformation within the already known quaternary structures T or R (Ackers, 1990).

Thermodynamic properties of the intermediate species have subsequently been correlated with an extensive variety of probes (Daugherty et al., 1991; Ackers et al., 1992; Doyle & Ackers, 1992; LiCata et al., 1993) which indicate the third allosteric state to be a form of the quaternary T molecule in which the additional energetic effect arises from ligand-induced tertiary conformational changes rather than by global alteration of the dimer–dimer interface. These studies have led to the proposal of a symmetry rule for distribution of the 10 ligation species among the two quaternary structures: switching from quaternary T to quaternary R occurs when ligation creates a tetramer with at least one ligand bound on each dimeric half-molecule, i.e., $\alpha^1\beta^1$ or $\alpha^2\beta^2$. Terminology of quaternary structural transition in this paper will refer to the global (T to R) reorientation of the $\alpha\beta$ dimers that accompanies complete heme site ligation (Baldwin & Chothia, 1979). Recent crystallographic work (Smith et al., 1991; Silva et al., 1992; Smith & Simmons, 1994) has demonstrated a third quaternary structure ("quaternary Y") which is accessible to fully-ligated hemoglobin. Conclusions of the present work would not be altered whether the fully-ligated CN-met tetramers are in quaternary Y or quaternary R. Additional studies have shown that the enthalpic and entropic components of cooperative free energy differ among the 10 ligation species in a manner that coincides with predictions of the symmetry rule (Huang & Ackers, 1993), and the same is found for linkage to NaCl (Ackers and Koestner, unpublished).

Transduction of Binding Energy into Hemoglobin Cooperativity. From the work mentioned above, a mechanistic understanding has emerged regarding the general nature of hemoglobin's "homotropic" allosteric interactions, i.e., for transduction of heme site binding into the tertiary and quaternary transitions. These mechanistic features (summarized below) provide a framework for understanding the roles of heterotropic effectors, including Bohr protons, which are analyzed in both the present study and the parallel study by Perrella et al. (1994).

(1) Binding the first heme site ligand induces alterations in tertiary conformation which are accompanied by the free energy penalty $^{ij}\Delta G_c$ defined above (eq 1). This unfavorable "tertiary constraint" energy that we shall denote by ΔG_{tc} opposes the "intrinsic" binding energy as illustrated in Figure 2. Species [11], [12], and [21] have the quaternary T structure (Daugherty et al., 1991; Ackers et al., 1992; LiCata et al., 1993), so that ΔG_{tc} reflects ligand-induced conformational

work performed against the quaternary T interface which serves as a mechanical constraint. This tertiary constraint effect simultaneously involves both α and β subunits within the dimeric half-molecule: binding the first ligand (either to α or to β) alters the affinity for ligating the other subunit. Hemoglobin thus exhibits cooperative binding within its quaternary T structure, which is paid for by the difference between conformational work induced upon binding the first subunit and that induced by ligating the second subunit within the same $\alpha\beta$ half-tetramer.

(2) The tertiary constraint energy and the intradimer cooperativity within T are not paid for by the breaking of noncovalent bonds of the dimer–dimer interface (LiCata et al., 1993). The argument for this point is as follows: (a) The magnitude of ligation-induced tertiary constraint is not affected by mutationally-altered residues of the adjacent dimer within a quaternary T tetramer, including those associated with salt bridges and hydrogen bonds of the dimer–dimer interface. (b) If ligating an α^1 or β^1 subunit in the normal tetramer breaks these bonds for which the energy of breakage is ΔG_{tc} (or a significant fraction thereof), then the numerical value of ΔG_{tc} should be altered when the "acceptor residues" on the adjacent dimer have been modified so that bond formation is precluded. The finding of energetic independence between modifications of such interfacial residues on one dimer and heme site ligation of the adjacent dimer (LiCata et al., 1993) thus argues against an energetic contribution to ΔG_{tc} from ligand-induced breakage of the noncovalent bonds associated with those residues.

(3) Only one of the dimers within a quaternary T tetramer can manifest tertiary constraint. The T interface cannot easily accommodate two such conformationally-perturbed dimers. Hence, the R interface is favored by molecules that are ligated on both the $\alpha^1\beta^1$ and $\alpha^2\beta^2$ dimers.

(4) When the molecule switches from T to R, it releases the unfavorable ΔG_{tc} stored earlier but expends an additional positive free energy through breaking salt bridges and other noncovalent bonds at the interface. Since this energy of T $\rightarrow$ R transition is larger (i.e., more positive) than ΔG_{tc}, the system experiences a second positive increment ($\Delta G_{T-R} - \Delta G_{tc}$) of cooperative free energy at each of the six switchpoints specified by the symmetry rule. The energy-generating effects of tertiary constraint and quaternary switching are thus distributed through the cascade of binding pathways. Additional cooperativity arises within the quaternary R structures as a result of quaternary enhancement, i.e., the affinity at the last step exceeds that of the intrinsic (dimer) value.

It is self-evident that these features of the allosteric mechanism could not have been deduced from properties of the end-state species nor the stepwise averages alone.

Coupling to Bohr Protons. Major features of the hemoglobin allosteric mechanism may be analyzed through the proton-binding and -release reactions which accompany heme site ligation and quaternary assembly (dimers to tetramers). While the tetrameric molecule has approximately 182 ionizable amino acid side chains (Matthews et al., 1985), only a much smaller subset of residues contributes significantly to the alkaline Bohr effect (pH 7–9.5). Their cumulative contribution upon complete oxygenation comprises slightly over 2 mol of H^+ released per tetramer at pH 7.4. Much discussion has centered around questions of which exact residues participate in this effect, how they are controlled by the tertiary and quaternary structural transitions and their energetic contributions (e.g., Perutz, 1970; Perutz et al., 1974; Szabo & Karplus, 1972; Ackers, 1980; Johnson et al., 1984; Matthews et al., 1985; Ho & Russu, 1987; Lee & Karplus, 1983; Lee et al., 1988; Riggs, 1988). Of importance to mechanistic understanding has been the question of how Bohr proton release is distributed with respect to the heme site-binding steps. Initial suggestion of a linear stepwise distribution (Wyman, 1948) has been found not to be correct (Imai & Yonetani, 1975; Chu et al., 1984; Lee et al., 1988).

A previous study from this laboratory (Chu et al., 1984) has determined model-independent relationships between stepwise release of oxygen-linked protons for tetramers and dimers and their contributions to the energetics of cooperativity over the pH range 7.4–9.5. This approach is extended in the present study to elucidate the relationships between free energies of the nine Bohr effects of the CN-met system. Although it is not feasible to determine the individual species Bohr effects by directly measuring proton release upon cyanomet ligation, we have been able to deduce equivalent information by characterizing the pH dependence of the quaternary assembly reactions (i.e., dimers into tetramers) for each of the ligation species (Figure 1) and utilizing the linkages between subunit assembly and heme site ligation.

One of the initial lines of evidence for assignment of the half-ligated species [21] molecule to quaternary T was the comparison of its energetic response to protons with properties of the deoxy species [01] and the fully-ligated species [41] (Daugherty et al., 1991). The work described in this paper extends that database to include each of the 10 ligation species of Figure 1 over the range from pH 7.0 to 9.5. Comparison of assembly free energies at each overall degree of ligation (i.e., molecules with zero, one, two, three, or four ligands bound) for cyanomet and oxygen ligation measured under identical conditions (Chu et al., 1984) suggests that coupling between heme site ligation and proton ionization may have common mechanisms in the two ligation systems.

Previously we studied O_2 binding onto vacant sites of the CN-met intermediates in order to explore combined effects of the two ligands (Doyle & Ackers, 1992). The results showed cooperative free energy distributions in correspondence with symmetry rule predictions, in spite of different energetic penalties generated by the two ligands for some of the microstates. Replication of that study at a series of pH values would in theory yield the corresponding Bohr proton releases for the mixed O_2–CN-met system. We have chosen, however, to use CN-met as the sole heme site ligand to avoid proton linkages of the (small) mixed-ligand discrepancies as well as difficulties achieving O_2 equilibrium that were found in the above-referenced study.

A parallel study (Perrella et al., 1994) has analyzed the CN-met ligation species by measuring protons released upon oxygenation of the vacant sites. The two studies are thus complementary and provide new information regarding the correspondence between O_2 ligation and CN-met ligation. The current database, in conjunction with recent studies on the energetic perturbations arising from single-site mutations in ligation species [01], [21], and [41] (LiCata et al., 1993), allows us to assess structural pathways at the level of tertiary vs quaternary transitions for the cooperative free energies and the sequence of Bohr proton release.

MATERIALS AND METHODS

Hemoglobins A and S were purified by the method of Williams and Tsay (1973). Cyanomethemoglobins and chains were prepared according to the following protocol. Concentrated oxyhemoglobin samples were oxidized by incubation with a 10% mol excess of $K_3Fe(CN)_6$ for 3 min at room

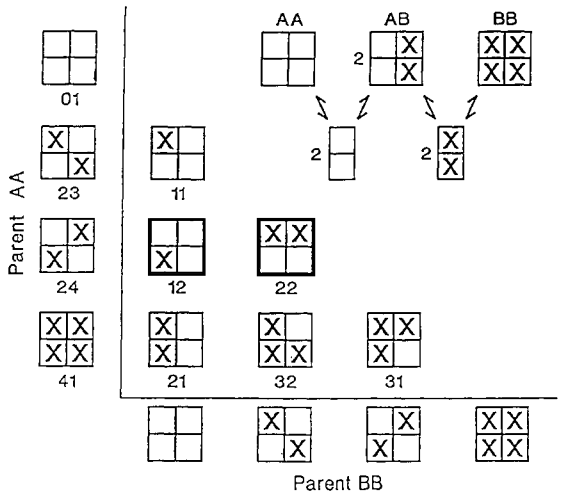

FIGURE 4: Hybridization scheme for the six asymmetric microstates. Reaction of 1 mol of dimer A and 1 mol of dimer B to form the hybrid tetramer AB from the parent tetramers AA and BB occurs by the dissociation–reassociation reaction diagrammed in the upper right corner.

temperature. This was followed by addition of a 10% mol excess of KCN and incubation for a further 3 min at room temperature to ligate the oxidized sites. (Stock solutions of $K_3Fe(CN)_6$ and KCN were 1 M.) The sample was immediately diluted by a 3-fold volume excess of cold buffer and run over a Sephadex G-50 column or centrifuged at 4 °C using Centricon 30 (Amicon) units to remove excess oxidant and exchange into standard buffers (Johnson, 1990). Samples prepared in this manner were spectrally assessed to be fully cyanomet and ran as a single band on isoelectric tubes. Samples that were incubated in the presence of oxidant for longer times resulted in several bands on the isoelectric focusing tubes. Hemoglobin species [23] $(\alpha^{+CN}\beta)(\alpha^{+CN}\beta)$ and [24] $(\alpha\beta^{+CN})(\alpha\beta^{+CN})$ were prepared by the method of Blough and Hoffman (Blough & Hoffman, 1984).

Standard buffers were either 0.1 M Tris-HCl (pH 7.0–8.5) or 0.1 M glycine (pH 8.8–9.5) with 0.1 M NaCl, 1 mM Na_2-EDTA, and 10 mM KCn at 21.5 °C. Trizma base, glycine, Na_2EDTA, and NaCl were from Sigma. KCN was from Fisher and $K_3Fe(CN)_6$ from VWR. Concentrations of total chloride ranged from 0.13 M (pH 8.5) to 0.19 M (pH 7.0). Free energies of ligation and assembly are insensitive to variations within this range (Doyle & Ackers, 1994).

Because of the dimer to tetramer equilibrium reaction, only four of the 10 ligation species of tetrameric hemoglobin can be isolated and studied in pure form. These are species [23] $(\alpha^{+CN}\beta)(\alpha^{+CN}\beta)$, species [24] $(\alpha\beta^{+CN})(\alpha\beta^{+CN})$, and the two end-states [01] $(\alpha\beta)(\alpha\beta)$ and [41] $(\alpha^{+CN}\beta^{+CN})(\alpha^{+CN}\beta^{+CN})$. Through various combinations of the constituent dimers from these four species, the remaining six species were formed and studied as a hybrid in a mixture that also contains the two parent species (Figure 4). Assembly free energies for the ligation states were determined by kinetic techniques (Smith & Ackers, 1985), analytical gel chromatography (Ackers, 1970; Valdes & Ackers, 1979), and quantitative cryogenic isoelectric focusing (Perrella & Rossi-Bernardi, 1981; LiCata et al., 1990).

Analytical Gel Chromatography. AGC was used to obtain assembly free energies for species [41], [23], and [24] under anaerobic conditions using the "large zone" technique. A zone of protein is passed through a Sephadex G-100 column to obtain a plateau region of constant protein concentration vs eluted volume. In subsequent experiments, one changes the total (plateau) hemoglobin concentration, C_T, and the equilibrium between dimers and tetramers shifts according to the law of mass action. The centroid position (equivalent sharp boundary) of the leading (or trailing) edges of each zone is analyzed to obtain the elution volume, V_{el}.

$$V_{el} = \int_0^{C_T} V dC \tag{2}$$

V_{el} is related to a weight average partition coefficient, σ_w, for the system.

$$\sigma_w = \frac{(V_{el} - V_o)}{V_i} \tag{3}$$

where V_o is void volume and V_i is internal volume of the gel. C_T is total concentration of protein. σ_w measures the average degree of solute penetration within the gel's interior solvent region and reflects the weight average of the species partition coefficients, i.e., dimers (σ_D) and tetramers (σ_T).

$$\sigma_w = \sigma_D f_D + \sigma_T f_T \tag{4}$$

where σ_D and σ_T are the molecular size-dependent partition coefficients for dimers and tetramers and f_D and f_T are respective fractions of the two species [cf. Ackers (1970)].

The partition coefficient for hemoglobin undergoing reversible dimer to tetramer assembly can be written as:

$$\sigma_w = \sigma_D\left[\frac{[(\alpha\beta)X_i]}{C_T}\right] + 2\sigma_T {}^{ij}K_2\left[\frac{[(\alpha\beta)X_i]^2}{C_T}\right] \tag{5}$$

where $[(\alpha\beta)X_i]$, $i = 1, 2$, is the concentration of ligated dimer and ${}^{ij}K_2$ is the equilibrium constant for forming tetrameric species $[ij]$ from its constituent dimers. These experiments were performed under anaerobic conditions to determine ${}^{ij}K_2$ and the Gibbs free energies of assembly for [23] and [24] using a Coy Laboratory type B anaerobic chamber as described elsehwere (Doyle & Ackers, 1992). Nonlinear regression (Turner et al., 1981) was used to estimate σ_D, σ_T, and ${}^{ij}K_2$.

Kinetic Technique. The rate constant, k_r, for dissociation of tetramer (T) to dimers (D) was determined using the haptoglobin kinetic technique. (Ip & Ackers, 1976; Turner et al., 1981; Speros et al., 1990). Haptoglobin binds rapidly to the dimers and traps them while the extent of dissociation vs time is monitored at 430 nm. With multiple species, the absorbance change is expressed as a sum of first-order rate processes:

$$A_{(t)} = A_\infty + P_1 e^{-k_1 t} + P_2 e^{-k_2 t} \tag{6}$$

For a hybrid mixture, the absorbance change is expressed as a sum of rate constants for the parents and the hybrid (Smith & Ackers, 1985).

$$A_{(t)} = A_\infty + P_1 e^{-k_{AA} t} + P_2 e^{-k_{AB} t} + P_3 e^{-k_{BB} t} \tag{7}$$

The rate constant for dimer to tetramer association, k_f, has been found to be invariant at 1.1×10^6 M^{-1} s^{-1} for normal, mutant, and chemically-modified hemoglobins (Pettigrew et al., 1982; Turner et al., 1992) and over the pH range 7.2–9.5 (Chu & Ackers, 1981). The equilibrium constant is calculated as ${}^{ij}K_2 = k_f/k_r$.

Quantitative Cryogenic Isoelectric Focusing. QCIEF is an equilibrium method to determine assembly free energies for the six species that must be studied as hybrids (Perrella & Rossi-Bernardi, 1981; Perrella et al., 1990; LiCata et al., 1990). Our version of the technique (LiCata et al., 1990) has

been modified as follows: in separate vials, parent hemoglobin samples and components of the oxygen-scavenging enzyme systems (described below) were deoxygenated on ice using a gentle flow of humidified nitrogen. In a glovebag, the two parent hemoglobins, at concentrations where tetramers are the predominant species, were mixed together and an oxygen-scavenging enzyme system was added. These enzyme systems were necessary to maintain anaerobicity of the samples during a wide variety of times for attaining equilibrium (i.e., from several minutes to >120 h). Three systems were used over the pH range investigated: (1) 5% v/v Oxyrase (Oxyrase Inc., Ashland, OH), an oxygen-scavenging system which uses lactate (1.5 mM final concentration) as substrate (Sigma, catalog no. L-1750). This system is active from pH 7.0 to 9.5. (2) Bovine catalase (Boehringer Mannheim, catalog no. 106810) at 0.6 mg/mL for pH 7.0 and 7.4. Or (3) for pH 8.0 and above, 0.6 mg/mL aspergillus niger catalase (Sigma, catalog no. C3515) with 1.8 mg/mL glucose oxidase (Sigma, catalog no. G2133) and 0.6% β-D-glucose (Sigma) was added to the hemoglobin samples. Tests of overlapping conditions yielded identical results with the various enzyme systems. Samples were distributed into small vials and incubated at the condition of interest until equilibrium was attained. In order to further maintain anaerobicity, all sample vials were immersed in larger vials containing a solution of sodium dithionite in deoxygenated H_2O (Johnson, 1990). This is found to be crucial when incubating samples longer than ~12 h. Upon attainment of equilibrium, the reaction was rapidly quenched into a (50/50) mixture of ethylene glycol and standard buffer at −25 °C. This halts rearrangement of the three tetrameric species. Samples were loaded onto poly(acrylamide) isoelectric focusing tube gels (pH range 6–8). Electrophoresis at −25 °C separates the three tetrameric species according to pI values. The tubes were scanned at 420 and 540 nm. Figure 5 shows representative scans at equilibrium time points for [21] at pH 7.4 and 9.5 and for [22] at pH 9.5. Even at extreme conditions (long incubations or high pH), sample integrity was not compromised, resulting in three unique peaks corresponding to the three tetrameric species in the reaction. Areas under these three peaks are related to the fractions of tetrameric species in the equilibrium mixture. These areas yield the deviation free energy, δ, calculated by

$$\delta = -RT \ln\left(\frac{f_{AB}}{2\sqrt{f_{AA}f_{BB}}}\right) \quad (8)$$

where f_{AA}, f_{BB}, and f_{AB} are the fractional populations of the three tetramers. The assembly free energy of the hybrid AB is calculated from

$$\delta = \Delta G_{AB} - 1/2(\Delta G_{AA} + \Delta G_{BB}) \quad (9)$$

Assembly free energy values of the parent species AA and BB were independently determined by the kinetic and analytical gel chromatography methods outlined above.

RESULTS

Table 1 lists the dimer–tetramer assembly free energies obtained experimentally over the pH range 7.0–9.5. The values in each column show how ligation at the heme sites controls the strength of the dimer–dimer interface at each proton chemical potential. Reciprocally, Figure 6 shows how the free energy of dimer–dimer interaction is controlled by

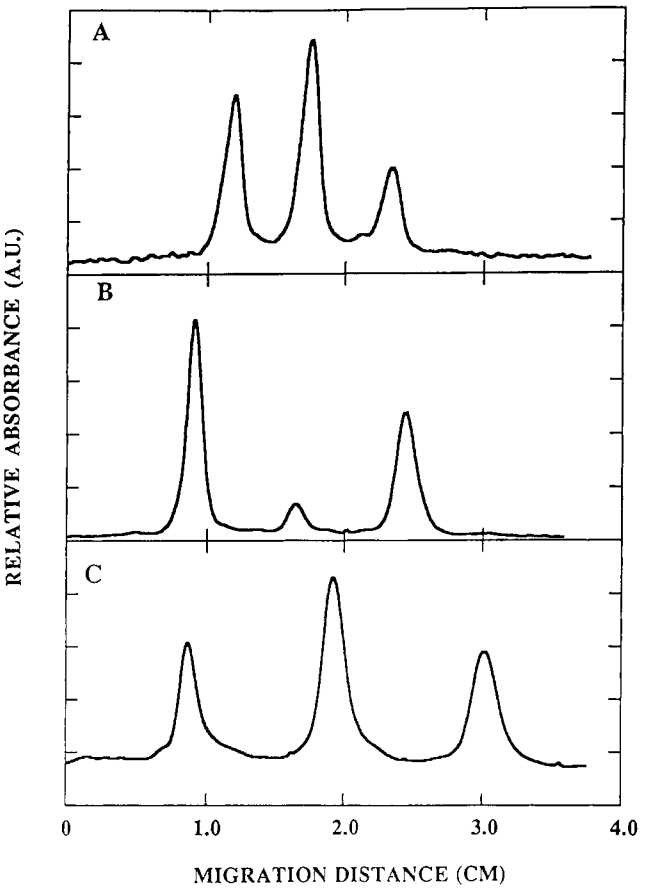

FIGURE 5: Representative scans from the quantitative cryo-isoelectric focusing technique. (A) Species [21] at pH 7.4 quenched after 178 h of incubation in the presence of the enzyme system 2 (see text for designation). Parent samples were cyanometHb A_o and deoxyHb S_o: δ = 0.13 kcal for this scan. (B) Species [21] at pH 9.5 quenched after 2.25 h of incubation in the presence of enzyme system 1. Parent samples were cyanometHb A_o and deoxyHb S_o: δ = 1.25 kcal for this scan. (C) Species [22] at pH 9.5 quenched after 3.75 h of incubation in the presence of enzyme system 3: δ = 0.11 kcal for this scan. Parent species were [24] made with Hb S_o β chains and [23]. All scans are at 420 nm.

chemical potential of protons for each of the 10 ligation microstates.

Shapes of the pH Distributions. The 10 ligation species exhibit three characteristic profiles over the range of pH 7.0–9.5 as seen in Figure 6. The fully-ligated species [41] has a sharply-biphasic profile (with maximum at pH 8.5) that has been observed previously with oxygen (Atha & Riggs, 1979; Chu & Ackers, 1981). A nearly-identical biphasic profile shape is exhibited by each of the six CN-met species that have at least one ligated subunit on each (αβ) dimeric half-molecule, i.e., species [22]–[24], [31], [32], and [41]. For these species, there are two (opposite) effects of increasing proton concentration: quaternary assembly is enhanced by protons between pH 9.5 and 8.5 but is opposed by protons in the pH region 8.5–7.0. By contrast, unligated hemoglobin, i.e., species [01], shows only a monophasic profile where protons progressively augment quaternary assembly. The singly-ligated species [11] and [12] and the asymmetric doubly-ligated species [21] exhibit a third general shape which has a qualitatively-similar slope to that of species [01] in the high pH region (8.5–9.5) but a nearly level slope below pH 8.5, where quaternary assembly becomes nearly independent of protons.

These contrasting distributions of proton-driven energies (Table 1, Figure 6) are analyzed in subsequent sections of this

Table 1: Free Energies of Quaternary Assembly (Dimers to Tetramers) for the 10 Ligation States of CN-methemoglobin

tetrameric state [*ij*]	pH 7.0	pH 7.4[c]	pH 8.0	pH 8.5	pH 8.8	pH 9.0	pH 9.5
[01][a]	−14.77 ± 0.1	−14.35 ± 0.1	−13.99 ± 0.1	−13.27 ± 0.1	−12.74 ± 0.1	−12.35 ± 0.1	−11.69 ± 0.1
[11]	−10.90 ± 0.1	−11.15 ± 0.1	−11.14 ± 0.2	−10.94 ± 0.2	−10.01 ± 0.2		−9.06 ± 0.3
[12]	−10.97 ± 0.2	−10.89 ± 0.1	−11.02 ± 0.1	−10.69 ± 0.2	−10.00 ± 0.2		−9.09 ± 0.2
[21]	−11.11 ± 0.1	−11.14 ± 0.1	−10.84 ± 0.2	−10.41 ± 0.2	−9.74 ± 0.3	−9.30 ± 0.3	−8.98 ± 0.3
[22]	−7.28 ± 0.2	−8.03 ± 0.1	−8.85 ± 0.2	−9.30 ± 0.2	−8.89 ± 0.3		−8.26 ± 0.2
[23]	−7.26 ± 0.1	−8.38 ± 0.1	−9.10 ± 0.2	−9.60 ± 0.1	−9.10 ± 0.2		−8.60 ± 0.1
[24]	−7.41 ± 0.1	−7.92 ± 0.1	−8.74 ± 0.1	−9.11 ± 0.1	−8.88 ± 0.1		−8.14 ± 0.1
[31]	−7.32 ± 0.1	−7.97 ± 0.1	−8.81 ± 0.2	−9.27 ± 0.2	−8.94 ± 0.2		−8.39 ± 0.2
[32]	−7.29 ± 0.1	−8.24 ± 0.1	−8.99 ± 0.2	−9.55 ± 0.2	−9.07 ± 0.2		−8.62 ± 0.3
[41][b]	−7.66 ± 0.1	−8.34 ± 0.1	−9.10 ± 0.1	−9.60 ± 0.1	−9.22 ± 0.1	−8.99 ± 0.1	−8.82 ± 0.1

[a] Values for [01] are from Chu and Ackers (1981). [b] Values for [41] are from Turner (1989). [c] Values at pH 7.4 are from Huang and Ackers (1994).

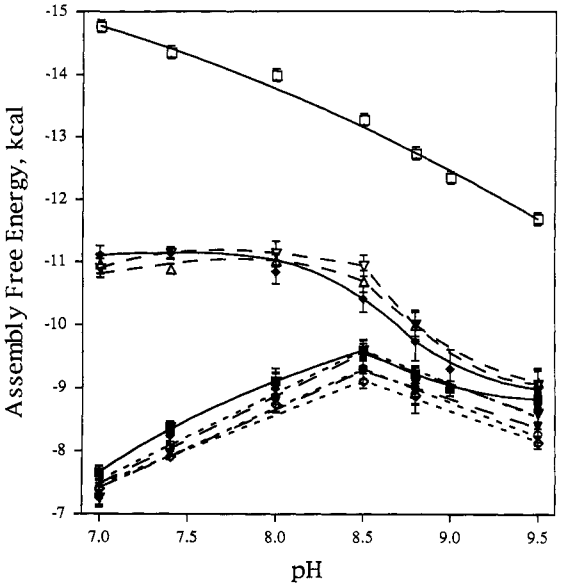

FIGURE 6: Distribution of assembly free energies for the 10 CN-met ligation microstates as a function of pH. Species [01] is represented by open squares and species [41] by closed squares (bottom curves). In the middle set of curves, down triangles are species [11], up triangles are species [12], and filled diamonds are species [21]. The remaining five microstates distribute closely in the bottom set of curves; the three remaining doubly-ligated species are indicated by dotted lines and the triply-ligated species by dashed lines.

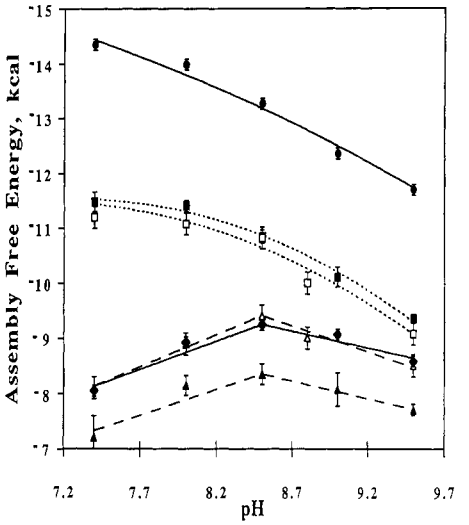

FIGURE 7: pH dependence of ligation-linked subunit assembly for oxyHb (filled symbols) compared with that for cyanometHb (open symbols). Circles, species [01]; squares, singly-ligated stage; triangles, triply-ligated stage; diamonds, species [41].

paper to evaluate the energetics and numbers of Bohr protonrelease and to compare these with corresponding properties of oxygenated hemoglobin.

A notable feature (Figure 6) is the close spacing between species [21] and the singly-ligated species [11] and [12], since this implies that their cooperative free energy values, ${}^{ij}\Delta G_c$, are nearly the same (Smith & Ackers, 1985). Thus, at each pH, the "free energy penalty" for ligating both sites on species [21] is essentially paid upon ligating the first site. At pH 8.8, for example (Figure 3, Table 1), the free energy of forming species [21] differs by 3.0 kcal from the sum of intrinsic ΔG_α and ΔG_β values as indicated in Figure 2. Whereas ligating only the α subunit (to form species [11]) costs 2.7 kcal, the remaining β subunit within the same $\alpha\beta$ half-tetramer is ligated with energy ($\Delta G_\beta + 0.3$). This translates into a 60-fold higher affinity than for ligating the β subunit alone (i.e., to form species [12]). Thus it is seen that even when energetic spacings for quaternary assembly are small between the "intermediate" and "quaternary R" profiles (Figure 6), the first two binding steps (to form species [21]) remain highly cooperative.

Figure 7 compares the assembly free energy distributions between oxygen and cyanomet systems for various stages of ligation. Over the pH range 7.4–9.5, the average assembly free energy of species [11] and [12] of cyanomethemoglobin shows very good agreement with values determined under these same experimental conditions for hemoglobin singly-ligated with oxygen. The magnitude of proton coupling to quaternary assembly for the singly-ligated species at pH 7.4 is found to be similar for the two ligation systems.

Due to suppression of the populations of doubly-ligated species during oxygenation, even their composite energetics cannot be resolved accurately from oxygen-binding data (Chu et al., 1984). At low pH, the average assembly free energy for the doubly-ligated oxygen species is suppressed compared to the cyanomet values. At high pH (>pH 8.5), the two systems appear to behave similarly [cf. Ackers et al. (1992)].

The pH profiles for the triply-ligated stage of both systems have the biphasic "signature profile" of quaternary R (Figure 7) and exhibit similar slopes. However the average free energy of assembly of [31] and [32] in the cyanomet system is ~0.9 kcal more favorable than that of the corresponding triply-ligated stage of the oxygen system at all pH values. While part of this difference is attributable to the difference in overall range between the two systems, a significant fraction is the quaternary enhancement effect (Mills & Ackers, 1979; Ackers & Johnson, 1990; Doyle & Ackers, 1992).

Overall, these results suggest that within each quaternary structure, the magnitude of assembly free energy for a given ligation species can be influenced by the type of heme site ligand but the coupling between heme site ligation and proton ionization follows the same mechanism in cyanomethemoglobin as in oxyhemoglobin. This correspondence is reinforced by the other analyses presented in this paper and the parallel study by Perrella et al. (1994).

Free Energies of the Nine Bohr Effects. For any ligation state, *ij*, the tetramer's affinity for heme site ligands and protons is mutually coupled to the free energies of quaternary assembly [cf. Chu et al. (1984)]. Thus the linkages between ligand binding, proton binding, and dimer to tetramer assembly permit us to delineate the energetic relationships between these coupled events for each of the nine ligated tetramers. To extract the Gibbs free energy of each Bohr effect, we consider first the following thermodynamic cycle:

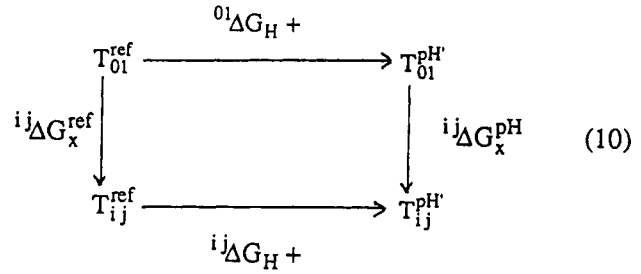

(10)

where T_{ij} is any one of the nine ligated tetramers and T_{01} is the unligated tetramer [01]. Subscripts denote binding of heme site ligands, X, or protons, H^+. The superscript "ref" denotes a pH where the tetramer Bohr effect vanishes, i.e., pH 9.5, under conditions of this study (Chu et al., 1984). The superscript pH′ indicates any other pH of interest. The upper and lower processes are thus proton titrations of species T_{01} and T_{ij} from the reference pH to pH′ where the free energy of the Bohr effect $^{ij}\Delta G_{Bohr}^{pH'}$ is

$$^{ij}\Delta G_{Bohr}^{pH'} = {}^{ij}\Delta G_{H^+} - {}^{01}\Delta G_{H^+} \quad (11)$$

The physical meaning of eq 11 is as follows. $^{01}\Delta G_{H^+}$ is the free energy of protonating the deoxy tetramer as it follows the titration path from "ref" to pH′. This term will include energetic contributions from reactions of protons with amino acid side chains plus all other ionic, solvation, or "structural effects" that may accompany the binding of protons to the deoxy tetramer. $^{ij}\Delta G_{H^+}$ is similarly the free energy of reacting species [*ij*] with protons along its titration curve and will similarly include contributions from other effects that accompany its reaction path. In general, the reactions at the top and bottom of eq 10 may differ energetically in contributions from both the local ionization energies and the other (structural) effects that accompany them. The quantity $^{ij}\Delta G_{Bohr}^{pH'}$ is their net free energy resultant.

Because ΔG is a state function, $^{ij}\Delta G_{Bohr}^{pH'}$ also equals the difference between free energies of heme site ligation (i.e., of forming species [*ij*] from species [01]) at the two pH values:

$$^{ij}\Delta G_{Bohr}^{pH'} = {}^{ij}\Delta G_X^{pH'} - {}^{ij}\Delta G_X^{ref} \quad (12)$$

Equations 11 and 12 illustrate the fact that the Bohr effect free energy is manifested identically whether the system is "probed" by heme site ligand or protons. Values of this function have been discussed previously for the overall oxygen-binding reactions over the same conditions as the present study (Chu et al., 1984).

The physical meaning of terms on the right of eq 12 is as follows. $^{ij}\Delta G_X^{ref}$ and $^{ij}\Delta G_X^{pH'}$ are free energies of heme site ligation to form species [*ij*] from the deoxy species [01] at the two pH values "ref" and pH′, respectively. In general, they include energetic contributions from ligation at each of the local heme sites, any accompanying tertiary and quaternary structural changes, the protons released (or absorbed) from amino acid side chains, and interactions with other ionic species and solvent, etc. Equation 12 also represents the area under the traditional curve of ligation-induced Bohr proton release when integrated from the reference pH (e.g., pH 9.5) as derived by Chu et al. (1984).

In order to extend this approach to the data of Table 1 for the nine ligation species of the present study, we may connect eq 12 with linkage eq 13 which pertains to any given pH:

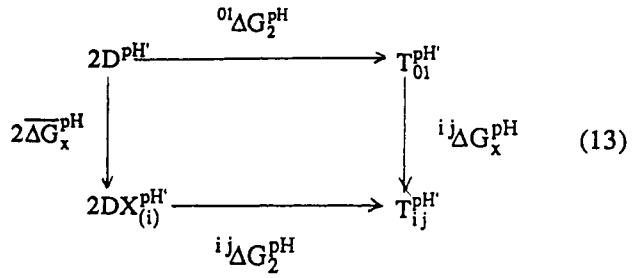

(13)

Reactions at the top and bottom depict assembly of tetramers [01] and [*ij*] from their constituent dimers, respectively. Those at the left and right depict ligation of the appropriate dimeric and tetrameric species: $DX_{(i)}^{pH}$ denotes the set of "constituent" dimers appropriate to the assembly of T_{ij} and $\overline{\Delta G}_X^{pH}$ is the mean ligation free energy for the two dimers. From eq 13, we have the following relationship at each pH:

$$^{ij}\Delta G_X^{pH} = {}^{ij}\Delta G_2^{pH} - {}^{01}\Delta G_2^{pH} + 2\overline{\Delta G}_X^{pH} \quad (14)$$

Writing one such relationship for pH′ and a second one for "ref", we may substitute for terms on the right side of eq 12 to obtain

$$^{ij}\Delta G_{Bohr}^{pH'} = (^{ij}\Delta G_2^{pH'} - {}^{ij}\Delta G_2^{ref}) - (^{01}\Delta G_2^{pH'} - {}^{01}\Delta G_2^{ref}) + 2(\overline{\Delta G}_X^{pH'} - \overline{\Delta G}_X^{ref}) \quad (15)$$

which upon rearrangement is equivalent to:

$$^{ij}\Delta G_{Bohr}^{pH'} - 2(\overline{\Delta G}_X^{pH'} - \overline{\Delta G}_X^{ref}) = (^{ij}\Delta G_2^{pH'} - {}^{01}\Delta G_2^{pH'}) - (^{ij}\Delta G_2^{ref} - {}^{01}\Delta G_2^{ref}) \quad (16)$$

We thus have expressions on each side of eq 16 for the Gibbs energy of ligation-induced proton release for each tetramer [*ij*] relative to a "dimer Bohr energy" term (i.e., on the left). The Bohr free energy of tetramers relative to dimers may thus be evaluated at each pH by using the experimental free energies given in Table 1 for terms on the right-hand side of eq 16. Results of these calculations are listed in Table 2 where the pH 9.5 data have been used as "reference".

It is found (Table 2) that the nine "difference Bohr energies" exhibit two values at each pH which distribute in a fashion that coincides precisely with predictions of the symmetry rule (Ackers et al., 1992). Species [11], [12], and [21] exhibit a common proton-linked free energy that is distinctly different in magnitude from a second value which is exhibited in common by the remaining six species, [22]–[24], [31], [32], and [41]. These results provide additional evidence for the symmetry rule. Taken together with the other lines of evidence (Ackers et al., 1992; Doyle & Ackers, 1992; LiCata et al., 1993; Huang & Ackers, 1994), we may identify the Bohr effect energy of species [11], [12], and [21] with a "tertiary Bohr effect" ΔG_{Bohr}^{tert} at each pH and that of the remaining species with a

Table 2: Gibbs Energies of Bohr Proton Release for CN-met Ligation of Tetramers Relative to Their Constituent Dimers[a]

tetrameric state [*ij*]	pH 7.0	pH 7.4	pH 8.0	pH 8.5	pH 8.8
[11]	1.24 ± 0.3	0.57 ± 0.2	0.22 ± 0.3	−0.30 ± 0.3	0.10 ± 0.3
[12]	1.20 ± 0.3	0.86 ± 0.2	0.37 ± 0.2	−0.02 ± 0.3	0.14 ± 0.2
[21]	0.95 ± 0.4	0.50 ± 0.3	0.44 ± 0.3	0.15 ± 0.4	0.29 ± 0.4
[22]	4.06 ± 0.3	2.89 ± 0.3	1.71 ± 0.3	0.54 ± 0.3	0.42 ± 0.3
[23]	4.42 ± 0.2	2.88 ± 0.2	1.80 ± 0.3	0.58 ± 0.2	0.55 ± 0.2
[24]	3.81 ± 0.2	2.88 ± 0.2	1.70 ± 0.2	0.61 ± 0.2	0.31 ± 0.2
[31]	4.15 ± 0.3	3.08 ± 0.3	1.88 ± 0.3	0.70 ± 0.2	0.50 ± 0.2
[32]	4.41 ± 0.3	3.04 ± 0.3	1.93 ± 0.4	0.65 ± 0.2	0.60 ± 0.3
[41]	4.24 ± 0.2	3.14 ± 0.2	2.02 ± 0.2	0.80 ± 0.3	0.65 ± 0.2
dimer terms[b]		−0.04 ± 0.3	−0.19 ± 0.3	−0.28 ± 0.3	0.11 ± 0.5

[a] Calculated according to eq 15 from the data of Table 1. [b] Values of $(G_X^{pH'} - \Delta\bar{G}_X^{ref})$ as given in eq 16 for oxygen binding to dimers [data of Chu et al. (1984)].

Table 3: Stepwise Gibbs Energies of Bohr Proton Release for O_2 and CN-met Ligation[a]

	ligation stages			
pH	0 → 1 CN (O_2)	1 → 3 CN (O_2)	3 → 4 CN (O_2)	0 → 4 CN (O_2)
7.4	0.72 (0.57)	2.4 (2.6)	0 (0)	3.1 (3.1)
8.0	0.29 (0.25)	1.7 (1.7)	0 (0)	2.0 (2.0)
8.5	0.16 (0.07)	0.64 (0.83)	0 (0)	0.8 (0.9)
8.95	0.12 (0.12)	0.48 (0.20)	0 (0)	0.5 (0.2)
9.5	0 (0)	0 (0)	0 (0)	0 (0)

[a] CN values are averaged over the ligation species (Table 2) at each stage of ligation. O_2 values are from Chu et al. (1984).

"quaternary Bohr effect" $\Delta G_{Bohr}^{T\rightarrow R}$ (arising from the T → R switchover). This behavior continues even at high pH (i.e., 8.8), where the free energies of species [11], [12], and [21] tend toward species [41] (Figure 6). Also listed in Table 2 are free energy contributions of the dimer terms to the Bohr energies for ligation with oxygen binding. These contributions are quite small compared with the tetrameric values. Although not measured for cyanomet ligation of dimers, the comparative overall results with oxygen (below) suggest that they are likely also to be small and constant (Doyle & Ackers, 1992).

Comparison of Stepwise Cyanomet Distribution with Oxygen. Table 3 shows the correspondence between free energies of the Bohr effect determined by the method described above for cyanomet ligation and oxygen binding. Over the pH range 7.4–9.5, the values obtained for dimer–tetramer assembly of the cyanomet species are found to coincide with corresponding values obtained by direct oxygen binding to tetramers (Chu et al., 1984). The average stepwise effects for the cyanomet intermediates show good correspondence with those from the oxygen system and are also in good agreement with the direct proton titration results of Antonini et al. (1965).

A traditional response function for representing the tetrameric Bohr effect is the plot of $\Delta\log P_m$ vs pH, where P_m is the concentration of dissolved oxygen at the median point of each saturation curve, expressed as partial pressure of a (hypothetical) equilibrated gas phase (Wyman, 1964). Since $\log P_m$ is proportional to the free energy of oxygen saturation $^{41}\Delta G_X^{pH'}$ of eq 12, we may relate $\Delta\log P_m$ ($= \log P_m^{pH'} - \log P_m^{9.5}$) to the proton-linked energy of ligand saturation at pH′, by means of eq 12:

$$^{41}\Delta G_{Bohr}^{pH'} = 4RT(2.303)\,\Delta\log P_m \qquad (17)$$

Then using eqs 14 and 16, we may transform the experimental assembly free energies (Table 1) for fully-ligated CN-methemoglobin into corresponding values of $\Delta\log P_m$ at each pH. In this calculation, we assumed the dimer Bohr energy terms for CN-met ligation to be the same as those for oxygenation, given in Table 2 (bottom). Values of $\Delta\log P_m$ obtained from the pH dependency of CN-met species [41] assembly vs that of unligated hemoglobin (Table 1) are shown in Figure 8 (open points). For comparison are plotted the values of $\Delta\log P_m$ obtained directly from oxygen-binding curves (closed circles) under the same experimental conditions (Chu et al., 1984). The two systems are thus found to exhibit the same magnitude and variation with pH in the response function, $\Delta\log P_m$. This suggests a fundamental similarity in overall mechanisms of coupling between heme site ligation and proton ionization, even though the detailed species distributions are known to be different (Ackers et al., 1992; Doyle & Ackers, 1993).

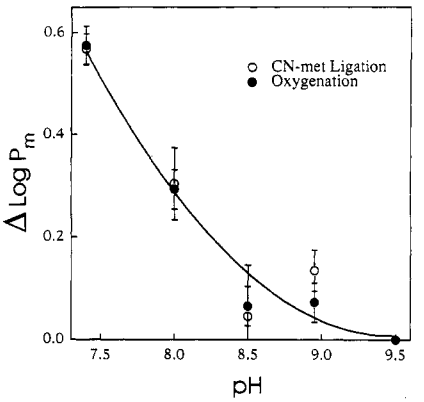

FIGURE 8: Response function for coupling of protons and heme site ligands (over all stages of binding). $\Delta\log P_m$ is the proton-induced shift (from pH 9.5) in median partial pressure of the oxygen saturation curve: open symbols, predicted from data of this study on cyanomethemoglobins, and filled symbols, experimentally observed for oxygen-binding curves obtained under identical conditions (Chu et al., 1984). pH dependence of the medians reflect proton coupling to the total ligation of all four sites.

Assembly Linkage to Proton Binding. The changes $^{ij}\Delta\nu_{H^+}$ in bound proton upon assembly of dimers into each tetrameric species [*ij*] were estimated using the well-known relationship (Wyman, 1964):

$$^{ij}\Delta\nu_{H^+} = \frac{1}{RT\ln 10}\frac{d(^{ij}\Delta G_2)}{d(pH)} \qquad (18)$$

The analysis is straightforward for the end-state species [01] and [41] and the intermediate species [23] and [24]. For the six species that must be studied as hybrid mixtures with their parents (i.e., [11], [12], [21], [22], [31], and [32]), the assembly free energy of the hybrid was calculated at each pH using eq 9.

Results were analyzed by Lagrange polynomials of degree 3 or 4 (Margenau & Murphy, 1956) with subsequent

Table 4: Protons Released upon Assembly and Heme Site Binding of CN-met or Oxygenated Species at pH 8.0

	(A) assembly-linked protons[a]			(B) ligation-linked protons[b]		
ligation species [*ij*]	${}^{ij}\Delta\nu_{H^+}^{CN}$	${}^{i}\Delta\nu_{H^+}^{O_2}$	(i_{O_2})	${}^{ij}\delta\Delta\nu_{H^+}^{CN}$	${}^{ij}\delta\Delta\nu_{H^+}^{O_2}$	(n_{O_2})
[01]	−0.83 ± 0.04	−0.83 ± 0.04	(0)			
[11]	0.21 ± 0.2	−0.49 ± 0.06	(1)	0.6 ± 0.2	0.3 ± 0.1	(1)
[12]	0.19 ± 0.1			0.6 ± 0.2		
[21]	−0.46 ± 0.1	nd	(2)	0.4 ± 0.2	1.2 ± 0.2	(2 + 3)
[22]	0.93 ± 0.1			1.8 ± 0.2		
[23]	1.0 ± 0.2			1.6 ± 0.2		
[24]	0.81 ± 0.1			1.6 ± 0.2		
[31]	0.81 ± 0.1	0.66 ± 0.09	(3)	1.6 ± 0.2		
[32]	0.92 ± 0.1			1.8 ± 0.2		
[41]	0.80 ± 0.1	0.48 ± 0.07	(4)	1.6 ± 0.2	1.3 ± 0.2	(4)

[a] Calculated from data shown in Figure 6 using eq 17. (i_{O_2}) = no. of oxygens bound/tetramer. [b] Difference Bohr effect (tetramers minus dimers) from eq 19. (n_{O_2}) = binding steps (first, middle two, and last).

differentiation to obtain their slopes for use in eq 18. The resulting values of ${}^{ij}\Delta\nu_{H^+}$ are given in Table 4, for pH 8.0. Derivatives of the higher pH data sets were not sufficiently well-defined for this analysis due to complexity of shape and low density of data spacing (see Figure 6). Listed for comparison are the assembly-linked proton values for tetramers with corresponding total numbers, (i_{O_2}), of bound oxygens (Chu et al., 1984). These data were originally analyzed by a series of second-order polynomials for each ΔG vs pH curve using each pH as a new origin for recalculating coefficients so that the (nonconstant) series of derivatives would accommodate differing values of $\Delta\nu_{H^+}$ at each pH (Chu et al., 1984; see p 610). We have reanalyzed these oxygenation data by Lagrange polynomials (not shown) which yielded good agreement with the previously-reported values (Chu et al., 1984).

A large and similar range of assembly-linked protonation at pH 8.0 is found for the two ligands, i.e., from 0.8 mol of H^+ absorbed (deoxy) to ~0.5 mol released for the fully-ligated species. Both ligation systems show a shift to larger proton releases at the later stages of ligation. The CN-met species segregate into two values of proton release which are not synchronized with the number of ligands bound. At each pH, they distribute instead with predictions of the symmetry rule, i.e., the two values of assembly-linked proton release distribute into ligation states (11, 12, 21) vs (22, 23, 24, 31, 32, 41).

Proton Release upon CN-met Ligation. In order to transform the values of assembly-linked protons (Table 4) into corresponding ligation-linked changes in protonation (a traditional way of viewing the Bohr effect), we may use the following version of eq 13:

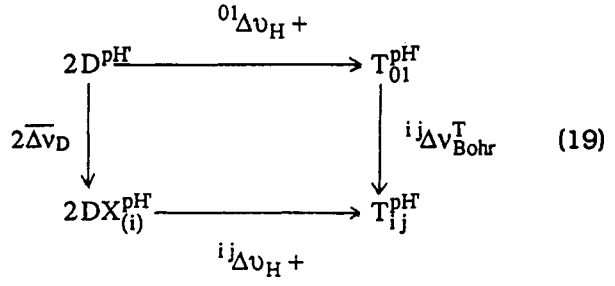

(19)

which shows dimer to tetramer assembly reactions (top and bottom) with their accompanying proton terms ${}^{ij}\Delta\nu_{H^+}$ and ${}^{01}\Delta\nu_{H^+}$. The traditional Bohr term for tetramer species [*ij*] is ${}^{ij}\Delta\nu_{Bohr}^{T}$, and for its constituent dimers, it is $2\Delta\bar{\nu}_D$. For this scheme, then:

$$ {}^{ij}\delta\Delta\nu_{Bohr} = ({}^{ij}\Delta\nu_{Bohr}^{T} - 2\Delta\bar{\nu}_D) = {}^{ij}\Delta\nu_{H^+} - {}^{01}\Delta\nu_{H^+} \quad (20) $$

Thus from values of Table 4A, we may calculate a *difference Bohr effect*, ${}^{ij}\delta\Delta\nu_{Bohr}$ (tetramer minus dimers), for each of the nine ligation species in the absence of knowledge regarding dimer Bohr effect values. This quantity, ${}^{ij}\delta\Delta\nu_{Bohr}$, is analogous to the cooperative free energy, ${}^{ij}\Delta G_c$, as it represents the increment in ligand-induced proton release that results from assembly of dimers into the tetrameric structure (correspondingly, ${}^{ij}\Delta G_c$ is the increment of ligand-induced free energy that results from assembly of the dimers into tetramers). If independent knowledge of the dimer Bohr effect's magnitude were available at each pH, we could of course calculate the tetramer value. This information is currently available only for oxygenation (Chu et al., 1984), where the dimer Bohr effect is also independent of the ligation step at each pH. With dissociated dimers, if one subunit (α or β) is ligated as CN-met, the other binds O_2 with a ΔG that is half the total value for binding O_2 at both sites (Doyle & Ackers, 1992). These results suggest similar properties for CN-met and O_2 binding to dimers.

Difference Bohr protons are given in Table 4B for the CN-met species at pH 8.0. Listed for comparison are the corresponding stepwise values for oxygenation, (O_2). As in the case of the assembly-linked proton values, there is good agreement between the overall difference Bohr effect for oxygens and CN-met, e.g., a total Bohr effect of 1.3 ± 0.2 mol at pH 8.0 corresponds to 1.6 ± 0.2 mol of H^+/4 O_2 bound, since a dimer Bohr effect of 0.07 mol of H^+/O_2 has been determined under these same conditions (Chu et al., 1984). The finding of similar values for the overall difference Bohr effect in the two ligation systems suggests that the dimer values for oxygen may be similar to those of CN-met dimers. The tertiary Bohr effect for ligation to form species [21] within the quaternary T structure may thus be estimated as 0.5 ± 0.3 mol of H^+ (i.e., 0.3 ± 0.2 mol of H^+ in excess of the dissociated dimer Bohr effect is found as an average of values for species [11], [12], and [21] of Table 4B). It is thus clear that the tertiary Bohr effect of the quaternary T tetramer shows a substantial enhancement over the Bohr effect present in dissociated dimers as was suggested by Lee and Karplus (1983). The corresponding Bohr effect for binding the first oxygen (0.4 ± 0.1 mol of H^+) appears slightly lower than the

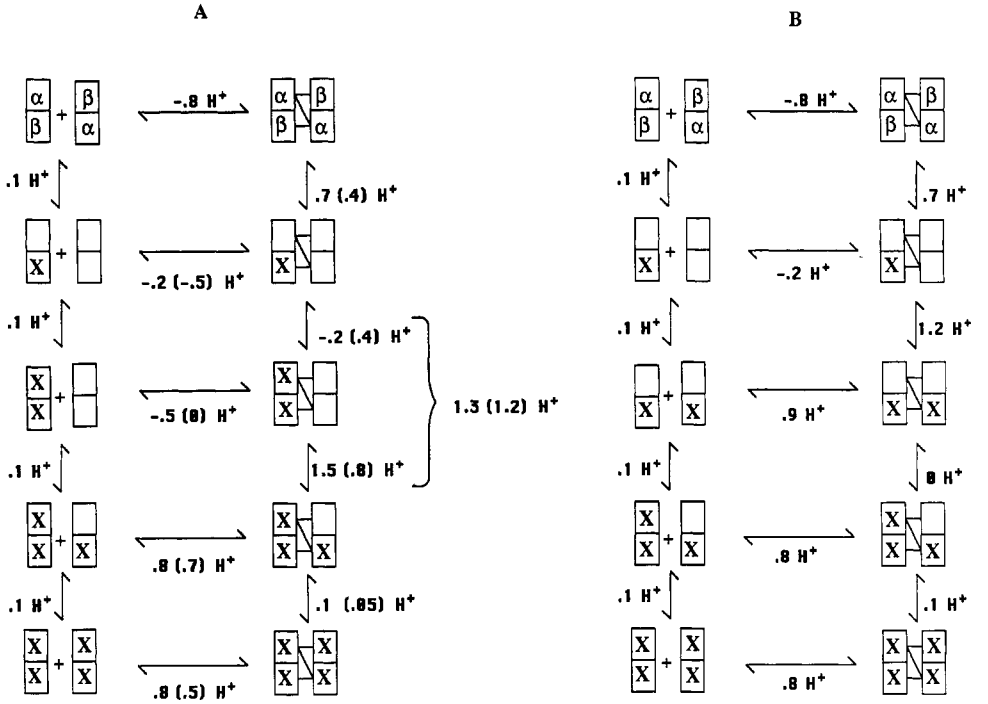

FIGURE 9: Proton linkage to assembly and ligation for representative pathways at pH 8.0. Values on the left are for CN-met ligation from this study. Values in parentheses are from the oxygenation studies of Chu et al. (1984) under identical conditions.

CN-met Bohr effect but cannot be distinguished within experimental error.

Symmetry Rule Behavior. A conspicuous feature of the distribution shown in Table 4B is that Bohr proton release shows correspondence with predictions of the symmetry rule. It is found that the tertiary Bohr effect accompanies almost entirely the first ligation within a dimeric half-tetramer in quaternary T. It thus parallels the appearance of "tertiary constraint free energy" which pays for the cooperativity in binding at both subunits within the dimeric half-tetramer (cf. LiCata et al., 1993; Figure 3). These relationships are summarized diagramatically in Figure 9 for two ligation sequences that represent alternative characteristic pathways with respect to symmetry rule behavior. This finding that essentially all of the tertiary Bohr protons are released at the first ligation step within the $\alpha\beta$ dimer is consistent with the earlier observation (Daugherty et al., 1991) that the ligand-induced tertiary constraint effect is manifested in CN-methemoglobin almost entirely at the first binding step.

DISCUSSION

Distribution of Species into Cooperative Free Energies. The most general distribution for the 10 ligation species of hemoglobin that embodies all the features observed to date is exemplified by the Co(II)/Fe(II)CO system (Speros et al., 1991) which shows five levels of cooperative free energy. In order to simultaneously accommodate the stepwise linkage data on oxygen binding to a normal hemoglobin, a minimum of five levels is also indicated (Ackers et al., 1992). The present results are consistent with the CN-met system being a "nearly-asymptotic form" of the five-level distribution in which the free energies of species [11], [12], and [21] are "condensed" into a single level and also where the quaternary enhancement effect (seen with normal oxygenated hemoglobin and the cobalt–iron–CO system) is negligible.

On the basis of the distributions found with the various heme site ligands and the correlation of their thermodynamic responses with quaternary structural probes, a "consensus" partition function, Ξ, has been proposed for the dominant terms of the hemoglobin allosteric mechanism (Ackers et al., 1992).

$$\Xi = 1 + 2K_{tc}(K_\alpha + K_\beta)X + [2K_\alpha K_\beta K_{tc}^{21} + 2K_\alpha K_\beta K'_{tc}K_c + K_\beta^2 K'_{tc}K_c + K_\alpha^2 K'_{tc}K_c]X^2 + [2K_\alpha K_\beta^2 K'_{tc}K_c + 2K_\alpha^2 K_\beta K'_{tc}K_c]X^3 + K_\alpha^2 K_\beta^2 K_c X^4 \quad (21)$$

K_α and K_β are intrinsic binding constants for ligand X on the α and β subunits, respectively. Within quaternary T are two "tertiary constraint" terms, K_{tc} and K_{tc}^{21}, which reflect the positive free energy ($\Delta G = -RT \ln K$) arising from ligation of each single subunit (α or β) or from both subunits of an $\alpha\beta$ dimer within the quaternary T tetramer. That K_{tc} may be different for the α and β subunits (Speros et al., 1991) is readily accommodated by slight extension of eq 21. Within quaternary R, there is a single tertiary constraint term, K'_{tc}, which reflects unfavorable energy arising from unligated subunits in the oxy quaternary structure. K_c represents the net free energy penalty for binding four ligands to deoxyhemoglobin (i.e., the net free energy of "structural rearrangement" that accompanies complete ligation). This partition function represents dominant relationships between the observed heme site ligation events and the major structural transitions. As such it provides a basic framework for further exploration. In general the various constants will have functional dependencies on allosteric effectors including pH, as illustrated by the present results.

The present study on CN-metHb with increased accuracy and range of data strongly suggests the same five-level distribution observed with the Co(II)/Fe(II)CO system (Speros et al., 1991) which is embodied in the partition function (eq 21). This is seen visually in Figure 3 for data at pH 8.8 where the species appear to distribute into five levels. At pH 8.0 and above, the experimental values distribute as follows: the first level is occupied by species [01], the singly-ligated species [11] and [12] distribute into a second level, species

[21] distributes into a third, while species [22]–[24], [31], and [32] distribute together, and species [41] occupies a fifth level. From pH 8.0 to 9.5, the average difference in tertiary constraint ΔG_{tc} between the singly-ligated species and species [21] is –0.25 kcal. Although this small difference barely exceeds the experimental error at any single pH, it is consistent over the pH range studied and is statistically significant.

The CN-met species [22]–[24], [31], and [32] have an average quaternary enhancement of 0.3 kcal from species [41]. Although small, this value is independent of pH and is statistically significant. The existence and magnitude of this effect have been confirmed by direct oxygen binding to the vacant sites of these five ligation species (Doyle & Ackers, 1992). At pH 7.4, an average 0.55 kcal of quaternary enhancement was found for binding the last O_2 to the triply-ligated cyanomet species and an average 0.22 kcal of quaternary enhancement for binding the last two oxygens to the doubly-ligated species [22]–[24]. The finding of this small but definite quaternary enhancement effect suggests once again that the cyanomet ligation system operates with the same basic mechanism as the oxygen system, even though magnitudes of the effects are slightly different.

High pH (pH 8.5–9.5)

A question arising from these results concerns the range of applicability of the symmetry rule. Does changing the chemical potential of protons alter the distribution of ligation species within a given quaternary structure? This is of particular interest at pH 9.5, where the assembly free energies of [11], [12], and [21] "coalesce" to within approximately 1 kcal of that of species [41] and where the Bohr effect vanishes. Are these species still quaternary T, have they switched to quaternary R, or are they an equilibrium mixture of T and R structures? If these three species (and indeed species [01]) have the R quaternary structure, then the combined absence of a tertiary Bohr effect that would have arisen from ligation within quaternary T and an absence of the ligand-induced T → R transition might result in a null Bohr proton release.

Indirect evidence however suggests that these species have a T quaternary structure and that the lack of Bohr proton release may arise from a near equivalence in the charge arrays for the T and R structures at pH 9.5. We find the cooperative free energies for species [11] and [12] to be nearly constant over the range of pH 7.4–9.5 (i.e., $\Delta G_c = 3.0 \pm 0.5$ kcal). Similarly, the cooperative free energy for species [21] shows only a small pH dependence from pH 7.4 to 9.5. At pH 7.4, these values reflect "tertiary constraint" arising from ligation-induced "conformational work" within the T quaternary structure (Ackers et al., 1992; LiCata et al., 1993). The similar cooperative free energy values at pH 9.5 suggest a common molecular basis. At pH 9.5, the distribution of assembly free energies appears within error to follow symmetry rule behavior. Formation of species [11], [12], and [21] is slightly more favorable than formation of [41]; species [22]–[24], [31], and [32] display small but significant quaternary enhancement effects. These two features of the energetic distribution suggest that the symmetry rule still holds at pH 9.5. It is easier to view these relationships at pH 8.8, where the overall cooperative free energy for [01] → [41] is greatly reduced from that at pH 7.4 but where discrete spacings of the cooperative free energy levels remain (Figure 3).

The Bohr Effect

Current understanding of the mechanism of the Bohr effect has been limited by the lack of experimental information on the roles of tertiary and quaternary structural changes in the cooperativity mechanism and also on the contributions of the various potential Bohr groups (Perutz, 1970). The present work, in conjunction with that described in the accompanying paper (Perrella et al., 1994) and with recent mutational studies (LiCata et al., 1993), indicates that the general pathway for Bohr proton release involves both a tertiary and a quaternary component and that these distribute according to the symmetry rule as depicted in Figure 9. On the basis of the assignment of species [21] to the quaternary T structure, it follows that the small but definite Bohr effect free energies for species [21] at each pH (Table 2) reflect proton release for dimeric half-tetramers upon ligand-induced tertiary change within the quaternary T structure.

Comparison with Results of Perrella et al. (1994). The results of this study, obtained solely with CN-met as ligand, are in general accord with those of Perrella et al. (1994) obtained using O_2 binding to the vacant sites of partially-CN-met species. Agreement is best at pH values greater than 7.5, where both studies support the operation of a symmetry rule. While possible sources of discrepancy between the methodologies have been noted (see the introduction), their relationship to the results obtained in the two studies is not easily defined. The least accurate results of the present study arise in the application of eqs 18–20 to obtain moles of Bohr protons from numerical differentiation of the CN-met dimer–tetramer assembly data; even though the Table 1 values that were differentiated are highly accurate, a greater density of pH spacing would be desirable. It was because of this uncertainty that we developed the Bohr free energy approach (eqs 12–16) which retains the high experimental accuracy. Thus the values of Table 2 establish on model-independent energetic grounds the linkages between protonation and heme site ligation with nearly the same accuracy as the primary data of Table 1 since they do not rely on applying polynomial or derivative relationships to the experimental points. Since the Table 2 values each represent the integral of Bohr proton release (from pH 9.5), it seems compelling that the clearcut symmetry rule distribution at each pH between 7.0 and 8.8 (Table 2) reflects the fundamental coupling between CN-met ligation and Bohr proton ionization. However, since values of Table 2 denote energies of tetramer Bohr protons minus energies of dimer Bohr protons, these values could have reduced sensitivity to a component of tetrameric Bohr proton release that hypothetically parallels the Bohr effect of dissociated dimers. Different dimer Bohr effects for CN-met and O_2 could thus contribute to the differences found in the two studies.

Relationship to Allosteric Models. It is of interest to consider briefly the relationships of several allosteric models to the findings of this study. The statistical thermodynamic model developed by Szabo and Karplus (1972) was expanded by Lee and Karplus (1983) to include a tertiary Bohr effect within quaternary T which exceeds the Bohr effect of dissociated dimers (Chu & Ackers, 1981) and arises from breaking salt bridges through ligand-induced tertiary structure change. The expanded model was found to be particularly consistent with pH-dependent oxygen-binding data of Poyart (Lee et al., 1988). Perutz has also proposed on the basis of MWC model parameters that the 0.6 mol of H^+ released at the first oxygen-binding step (at pH 7.4) in the data of Chu et al. (1984) is almost entirely a tertiary Bohr effect within quaternary T [Perutz (1989), see p 158] and suggested a breakage of salt bridges prior to quaternary switching. Applications of both the MWC and Lee–Karplus models thus correctly predicted the existence of a tertiary Bohr effect in

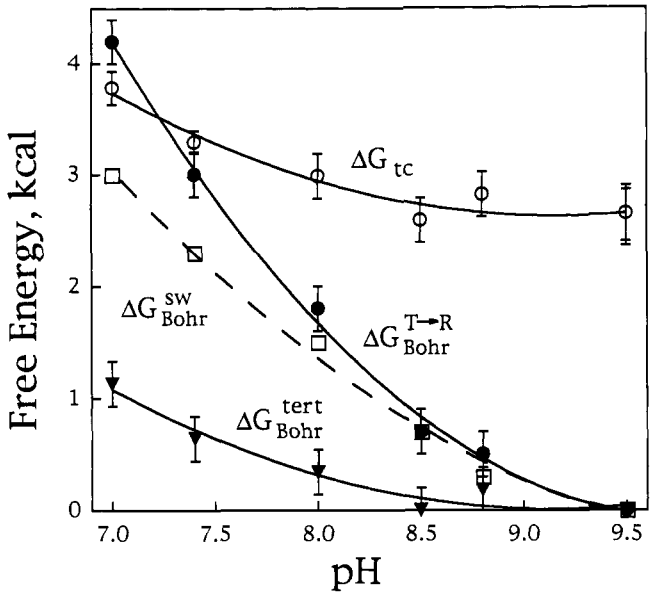

FIGURE 10: Energetic components of the Bohr effect for CN-methemoglobin. ΔG^{tert}_{Bohr}, free energy of ligation-linked proton release within the quaternary T molecule in excess of that for dissociated dimers; ΔG_{tc}, ligation-induced energy of tertiary constraint which is stored prior to the quaternary T → R switch; ΔG^{sw}_{Bohr}, proton-linked component of the switchpoint energy at each of the six switchpoints specified by the symmetry rule; $\Delta G^{T\rightarrow R}_{Bohr}$, free energy of Bohr proton release upon complete ligation relative to that for the same sites in dissociated dimers.

excess of the dissociated dimer Bohr effect, even though not accounting for symmetry rule behavior nor intradimer cooperativity within tetramers. Using an MWC–KNF hybrid model, Johnson et al. (1984) proposed that quaternary T → R switching should parallel the main component of Bohr proton release, assuming the observed dimer Bohr effect to equal the tertiary Bohr effect of tetramers and assuming KNF rules of ligand-linked pairwise subunit interactions (Koshland et al., 1966). Experimental findings of the present study show that quaternary switching does parallel the major component of Bohr proton release but does so in accord with symmetry rule behavior, intradimer cooperativity, and an enhanced tertiary Bohr effect that were not accounted for by the model of Johnson et al. (1984). These examples, comprising only a partial list, illustrate that such models, which are "for the most part, caricatures of reality" (Kac, 1969), may support, or suggest, features of a real system even with flawed or incomplete assumptions. They further illustrate the necessity of determining the intermediate-state properties by experimental methods.

Difference Bohr energies of several kinds are plotted in Figure 10. Tertiary Bohr energies, ΔG^{tert}_{Bohr}, are the averages at each pH over species [11], [12], and [21] as given in Table 2. Values for the total Bohr effect (averaged at each pH over the Table 2 values for species [22], [23], [24], [31], [32], and [41]) are plotted as $\Delta G^{T\rightarrow R}_{Bohr}$. Since ΔG^{tert}_{Bohr} is "released" upon rearrangement of the T → R interface, the net Bohr component ΔG^{SW}_{Bohr} which accompanies each of the six allosteric switchpoints (Ackers et al., 1992) was calculated as the difference between total and tertiary Bohr effects. Mean free energies of tertiary constraint ΔG_{tc} are plotted for comparison. It is seen that the pH dependency of ΔG_{tc} is accounted for by the tertiary Bohr energy, while ΔG_{tc} also contains a pH-independent part. It is thus seen that hemoglobin utilizes both a pH-dependent and a pH-independent component of cooperativity prior to the quaternary switch, as was suggested from computational modeling by Lee et al. (1988). The existence of a non-proton-linked component of cooperativity (e.g., mediated by quaternary switching) is dictated by the highly cooperative binding found with oxygen at pH 9.5 where no Bohr effect is present (Antonini et al., 1965; Chu et al., 1984; Lee et al., 1988). Such an effect is also manifested with CN-met ligation when the Table 2 data at pH 9.5 are converted into cooperative free energies by eq 1 (results not shown).

The structural origins of $\Delta G^{T\rightarrow R}_{Bohr}$ may be expected to include the alteration of proton-linked hydrogen bonds within the $\alpha^1\beta^2$ interface, including the classical salt bridges (Perutz, 1970). $\Delta G^{T\rightarrow R}_{Bohr}$ may also reflect the "distributed" (global) effects of altering the charge arrays of ionizable groups through quaternary reorientation. Structural origins of the tertiary Bohr effect are more difficult to assign in view of recent studies (LiCata et al.) which show that only negligible effects (i.e., less than 0.2–0.3 kcal) on ΔG^{tert}_{T} could arise from altering any of the interdimer salt bridges or hydrogen bonds. While none of the modified residues (including β146 His, β94 Asp, α141 Arg, and α40 Lys) affect ΔG_{tc} more than the 0.3 kcal error limits (at pH 7.4), it is possible that several of these groups might cumulatively generate the (1.1 ± 0.2 kcal) tertiary Bohr energy at pH 7.0 (Figure 10). Obvious candidates would include the salt bridges associated with the residues mentioned above. Other possible origins of the tertiary Bohr effect may include ligand-induced breakage of intradimeric salt bridges and conformational strain that could alter pK_a values of these (and other) ionizable groups without bond breakage.

ACKNOWLEDGMENT

This paper is dedicated to the memory of George Nemethy who made pioneering contributions to the understanding of allostery. He provided early encouragement to our work on hemoglobin's intermediate states. We thank Professor M. Perrella for help in our adaptation and use of powerful cryogenic techniques that he pioneered and for valuable discussions regarding the work presented in this paper.

REFERENCES

Ackers, G. K. (1970) *Adv. Protein Chem. 24*, 343–446.
Ackers, G. K. (1980) *Biophys. J. 32*, 331–343.
Ackers, G. K. (1989) *Biophys. Chem. 16*, 371–382.
Ackers, G. K., & Johnson, M. L. (1981) *J. Mol. Biol. 147*, 559–582.
Ackers, G. K., & Johnson, M. L. (1989) *Biophys. Chem. 37*, 265–279.
Ackers, G. K., Doyle, M. L., Myers, D., & Daugherty, M. A. (1992) *Science 255*, 54–63.
Antonini, E., Wyman, J., Brunan, M., Bucci, E., Franticelli, C., & Rossi Fanelli, A. (1965) *J. Biol. Chem. 240*, 1096–1103.
Atha, D. H., & Riggs, A. F. (1976) *J. Biol. Chem. 251*, 5537–5543.
Baldwin, J., & Chothia, C. (1979) *J. Mol. Biol. 129*, 175–220.
Blough, N. V., & Hoffman, B. M. (1984) *Biochemistry 23*, 2875–2882.
Chu, A. H., & Ackers, G. K. (1981) *J. Biol. Chem. 256*, 1199–1205.
Chu, A. H., Turner, B. W., & Ackers, G. K. (1984) *Biochemistry 23*, 604–617.
Daugherty, M. A., Shea, M. A., Johnson, J. A., LiCata, V. J., Turner, G. T., & Ackers, G. K. (1991) *Proc. Natl. Acad. Sci. U.S.A. 88*, 1110–1114.
Doyle, M. L., & Ackers, G. K. (1992) *Biochemistry 31*, 11182–11195.
Doyle, M. L., & Ackers, G. K. (1994) (in preparation).
Ho, C., & Russu, I. M. (1987) *Biochemistry 26*, 6299–6305.
Huang, Y., & Ackers, G. K. (1993) *Biophys. J. 64*, A44.

Imai, K., & Yonetani, T. (1975) *J. Biol. Chem. 250*, 2227–2231.
Ip, S. H. C., & Ackers, G. K. (1977) *J. Biol. Chem. 252*, 82–87.
Johnson, J. A. (1990) Ph.D. Dissertation, The Johns Hopkins University, Baltimore, MD.
Johnson, M. L., & Ackers, G. K. (1982) *Biochemistry 21*, 201–211.
Johnson, M. L., Turner, B. W., & Ackers, G. K. (1984) *Proc. Natl. Acad. Sci. U.S.A. 81*, 1093–1097.
Kac, M. (1969) *Science 166*, 695–698.
Kilmartin, J. V., Fogg, J. H., & Perutz, M. F. (1980) *Biochemistry 19*, 3189–3193.
Koshland, D. E., Nemethy, G., & Filmer, D. (1966) *Biochemistry 5*, 364–385.
Lee, A. W. M., & Karplus, M. (1983) *Proc. Natl. Acad. Sci. U.S.A. 80*, 7055–7059.
LiCata, V. J., Speros, P. C., Rovida, E., & Ackers, G. K. (1990) *Biochemistry 29*, 9772–9783.
LiCata, V. J., Dalessio, P. M., & Ackers, G. K. (1993) *Proteins 17*, 279–296.
Lee, A. W.-M., Karplus, M., Poyart, C., & Bursaux, E. (1988) *Biochemistry 27*, 1285–1301.
Margenau, H., & Murphy, G. M. (1956) *The Mathematics of Physics and Chemistry*, 2nd ed., Van Nostrand, New York.
Matthews, J. B., Gurd, F. R. N., Garcia-Moreno, E. B., Flanagan, M. A., March, K. L., & Shire, S. J. (1985) *CRC Crit. Rev. Bioch. 18*, 90–197.
Mills, F. C., & Ackers, G. K. (1979) *Proc. Natl. Acad. Sci. U.S.A. 76*, 273–277.
Monod, J., Wyman, J., & Changeux, J.-P. (1965) *J. Mol. Biol. 12*, 88–118.
Perrella, M., & Rossi-Bernardi, L. (1981) *Methods Enzymol. 76*, 133–143.
Perrella, M., Benazzi, L., Shea, M. A., & Ackers, G. K. (1990a) *Biophys. Chem. 35*, 97–103.
Perrella, M., Colosimo, M., Benazzi, L., Ripamonti, M., & Rossi-Bernardi, L. (1990b) *Biophys. Chem. 37*, 211–223.
Perrella, M., Davids, N., & Rossi-Bernardi, L. (1992) *J. Biol. Chem. 267*, 8744–8751.
Perrella, M., Schrager, R. I., Ripamonti, M., Manfredi, G., Berger, R. L., & Rossi-Bernardi, L. (1993) *Biochemistry 32*, 5233–5238.
Perrella, M., Benazzi, L., Ripamonti, M., & Rossi-Bernardi, L. (1994) *Biochemistry* (following paper in this issue).
Perutz, M. F. (1989) *Quart. Rev. Biophys. 22*, 139–236.
Perutz, M. F. (1970) *Nature 228*, 726–739.
Perutz, M. F., Ladner, J. E., Simon, S. R., & Ho, C. (1974) *Biochemistry 13*, 2163–2173.
Pettigrew, D. H., Romeo, P. H., Tsapis, A., Thillet, J., Smith, M. L., Turner, B. W., & Ackers, G. K. (1982) *Proc. Natl. Acad. Sci. U.S.A. 79*, 1849–1853.
Riggs, A. F. (1988) *Annu. Rev. Physiol. 50*, 181–204.
Silva, M. M., Rogers, P. H., & Arnone, A. (1992) *J. Biol. Chem. 267*, 17248–17256.
Smith, F. R., & Ackers, G. K. (1983) *Biophys. J. 41*, 415.
Smith, F. R., & Ackers, G. K. (1985) *Proc. Natl. Acad. Sci. U.S.A. 82*, 5347–5351.
Smith, F. R., & Simmons, K. C. (1994) *Proteins 18*, 295–300.
Smith, F. R., Gingrich, D., Hoffman, B., & Ackers, G. K. (1987) *Proc. Natl. Acad. Sci. U.S.A. 84*, 7089–7093.
Smith, F. R., Lattman, E. E., & Carter, C. W. (1991) *Proteins 10*, 81–91.
Speros, P. C., LiCata, V. J., Yonetani, T., & Ackers, G. K. (1991) *Biochemistry 30*, 7254–7262.
Szabo, A., & Karplus, M. (1972) *J. Mol. Biol. 72*, 163–197.
Turner, B. W., Pettigrew, D. W., & Ackers, G. K. (1981) *Methods Enzymol. 76*, 596–628.
Turner, G. (1989) Ph.D. Dissertation, The Johns Hopkins University, Baltimore, MD.
Valdes, R., Jr., & Ackers, G. K. (1979) *Methods Enzymol. 51*, 125–141.
Williams, R. C., & Tsay, K. Y. (1973) *Anal. Biochem. 54*, 137–145.
Wyman, J. (1948) *Adv. Protein Chem. 4*, 407–531.
Wyman, J. (1964) *Adv. Protein Chem. 18*, 223–285.
Yonetani, T., Yamamoto, H., & Woodrow, G. V. (1974) *J. Biol. Chem. 249*, 682–690.